



## ORIGINAL ARTICLE

# Establishment and characterization of a novel highly malignant lung cancer cell line ZX2021H derived from a metastatic lymph node lesion

Lingling Zu<sup>1,2,3</sup>  | Xuebing Li<sup>3</sup> | Jinling He<sup>3</sup> | Ning Zhou<sup>3</sup> | Fanrong Meng<sup>4</sup> | Xiaozhou Li<sup>4</sup> | Song Xu<sup>3</sup>  | Lei Zhang<sup>1,2</sup>

<sup>1</sup>School of Life Sciences, Tianjin University, Tianjin, China

<sup>2</sup>Tianjin Key Laboratory of Function and Application of Biological Macromolecular Structures, Tianjin University, Tianjin, China

<sup>3</sup>Tianjin Key Laboratory of Lung Cancer Metastasis and Tumor Microenvironment, Tianjin Lung Cancer Institute, Tianjin Medical University General Hospital, Tianjin, China

<sup>4</sup>Department of Obstetrics & Gynecology, Tianjin Medical University General Hospital, Tianjin, China

## Correspondence

Lei Zhang, School of Life Sciences, Tianjin University, Tianjin, China.  
Email: zhanglei@tju.edu.cn

Song Xu, Department of Lung Cancer Surgery, Lung Cancer Institute, Tianjin Medical University General Hospital, 154 Anshan Road, Heping, Tianjin 300052, China.  
Email: xusong198@hotmail.com

## Funding information

General Project of Tianjin Lung Cancer Institute, Grant/Award Number: TJLCS2021-03; Incubation Fund of General Hospital of Tianjin Medical University, Grant/Award Number: ZYFY2019022; Key Project of Cancer Foundation of China, Grant/Award Number: CFC2020kyxm003; Key Project of Tianjin Lung Cancer Institute, Grant/Award Number: TJLZD2021-05; National Natural Science Foundation of China, Grant/Award Number: 82172776; Startup Project of Tianjin Lung Cancer Institute, Grant/Award Number: TJLZJ2021-09

## Abstract

**Background:** Lung cancer is a highly malignant tumor with a poor prognosis. The establishment of faithful ex vivo cell models is essential for investigating the metastatic mechanisms and developing new anticancer agents. In this study, we established and characterized a novel lung cancer cell line derived from metastatic lymph node tissue from a Chinese patient.

**Methods:** A primary culture of metastatic lymph node tissue from a patient with lung cancer was used to establish a cell line. The phenotypic characteristics of the cell line were characterized by colony-formation, CCK8, and Transwell assays, and xenografting. The genetic characteristics were evaluated by chromosome analysis, short tandem repeat (STR) profiling, and quantitative real time-polymerase chain reaction (qRT-PCR).

**Results:** A novel lung cancer cell line, named ZX2021H, was successfully established from a metastatic lymph node lesion from a lung cancer patient. The cell line exhibited high capacities for proliferation and invasion, as validated by its phenotypic and genetic characteristics. This cell line had a unique STR profile and karyotype analysis revealed numerical and structural chromosome abnormalities. The growth rate of in vivo xenografted tumors established using ZX2021H cells was higher than that using H1299 cells. The cell stemness-related gene SOX2 was overexpressed in ZX2021 compared with H1299 cells, as determined by qRT-PCR.

**Conclusion:** We successfully established a novel, highly malignant lung cancer cell line, ZX2021H, derived from metastatic lymph node tissue from a Chinese lung cancer patient. This cell line may provide an ideal cell model for further studies of the molecular mechanisms underlying lung cancer metastasis and for the development of new anticancer agents.

## KEYWORDS

cell line, lung cancer, lymph node metastasis, primary culture

## INTRODUCTION

Lung cancer is a highly malignant tumor with the inherent biological properties of rapid proliferation and early spread, leading to a poor prognosis. Lung cancer is generally classified into two main histological types: small cell lung cancer

and non-small cell lung cancer (NSCLC), of which NSCLC accounts for approximately 85% of all cases.<sup>1-4</sup> Despite substantial progress in the treatment of NSCLC, including the advent of immunotherapy and various targeted therapies, the prognosis of patients with NSCLC remains poor and the 5-year overall survival rate is still <19%.<sup>5-7</sup> Tumor

This is an open access article under the terms of the Creative Commons Attribution-NonCommercial License, which permits use, distribution and reproduction in any medium, provided the original work is properly cited and is not used for commercial purposes.

© 2022 The Authors. *Thoracic Cancer* published by China Lung Oncology Group and John Wiley & Sons Australia, Ltd.

metastasis is the main reason for the high mortality of lung cancer; however, the molecular mechanisms underlying lung cancer metastasis remain unclear.<sup>8</sup> Further research into the mechanisms of tumor metastasis in lung cancer is therefore needed to develop effective treatment strategies.

Faithful *ex vivo* cell models are important tools for both basic and translational research. The SHP-77 cell line derived from a 54-year-old man by Fisher and Paulson<sup>9</sup> has been widely used for *in vitro* lung cancer studies.<sup>10–12</sup> The A549/cisplatin cell line was established by exposing A549 cells to gradually increasing cisplatin concentrations, and has been widely applied to investigate drug resistance mechanisms in lung cancer.<sup>13,14</sup> Zhou et al. modified and established the L9981 cell line for the study of lung cancer metastasis.<sup>15</sup> However, most lung cancer cell lines have been isolated and established from *in situ* lesions, thus potentially limiting their metastatic capacity.<sup>16–22</sup> Furthermore, Zou et al. showed that cells derived from metastatic lesions had stronger metastatic ability than cells from the corresponding primary tumor, both *in vitro* and *in vivo*.<sup>23</sup> There is therefore a need to establish a high metastatic potential lung cancer cell line derived from metastatic lesions as a suitable model for investigating the underlying metastatic mechanisms and ways in which to circumvent the potential metastasis risk.

In the present study, we established a novel NSCLC cell line, named ZX2021H, derived from metastatic lymph node tissue from a Chinese patient with advanced NSCLC. We investigated its morphology, proliferation, migration, and invasion *in vitro*, and determined its chromosomal characteristics, as well as its tumorigenic and metastatic capabilities *in vivo*, demonstrating its high malignant potential in lung cancer.

## METHODS

### Clinical information

The tumor specimen was sourced from a neck lymph node metastasis in a 42-year-old Chinese male patient diagnosed with lung adenocarcinoma at Tianjin Medical University General Hospital. The primary tumor was located in the lower right lung lobe. The patient received one cycle of chemotherapy (pemetrexed/cisplatin) and subsequently underwent right lower lobectomy and right supraclavicular lymph node dissection. Resected fresh metastatic lymph node tissue from the patient's neck was promptly harvested in the operating room. The study was conducted with the approval of the Ethics Committee of Tianjin Medical University General Hospital (Ethical No. IRB2022-WZ-026), and the patient signed the informed consent form.

### Primary tissue culture and establishment of a cell line

Resected metastatic lymph node tissue was subjected to primary culture to establish a cell line. Briefly, primary tissue

was minced using scissors and incubated successively with 0.2% collagenase II (Worthington) and 0.25% trypsin-EDTA (Gibco) for 30 min at 37°C. The reaction was terminated by adding McCoy's 5A medium with 10% fetal bovine serum (FBS; Gibco), and the dissociated tumor cells were then collected using a 70- $\mu$ m nylon mesh (BD Falcon). The cells were cultured in McCoy's 5A medium (Gibco) with 20% FBS, 100 U/ml penicillin-streptomycin (Gibco), 2 mM L-glutamine (Gibco), and 1 $\times$  nonessential amino acids (Gibco) in a 37°C incubator with 5% CO<sub>2</sub> and 95% air. When the cells reached 70%–80% confluency, they were split and inoculated into fresh McCoy's 5A medium at a ratio of 1:3. The medium was changed twice a week. After 6 months of repeated passaging, a new lung cancer cell line ZX2021H was successfully established. The following experiments were performed using passage 30 passage ZX2021H cells.

### Morphological observation and cell proliferation analysis

ZX2021H cells were seeded in a 60-mm dish and incubated at 37°C in a humidified atmosphere containing 5% CO<sub>2</sub>. The culture medium was changed every 2 days. When the cells reached 40%–50% confluence, their general morphology was observed under an inverted microscope, without staining. Cell proliferation was analyzed using a cell counting kit-8 assay (CCK-8; Dojindo), based on three independent experiments. The cells were seeded into 96-well culture plates at a density of 5  $\times$  10<sup>3</sup> cells/well and incubated at 37°C (5% CO<sub>2</sub>, 95% air) for 24, 48, 72, and 96 h. CCK-8 reagent (100  $\mu$ l of McCoy's 5A containing 10  $\mu$ l CCK-8 solution) was then added to each well for 3 h and the formazan level was quantified by measuring the optical density at 450 nm. Cell growth curves were constructed on the basis of absorbency and used to calculate the doubling time for ZX2021H cells.

### Migration and invasion assays

Cell migration and invasion were evaluated *in vitro* using Transwell chambers (Corning) according to the manufacturer's instructions. Cell suspensions (400  $\mu$ l, 3–16  $\times$  10<sup>4</sup> cells/well) were seeded into the upper chamber without Matrigel coating for migration assays, or with Matrigel coating for invasion assays, and 700  $\mu$ l culture medium with 10% FBS was added to the lower chamber, followed by incubation in a humidified incubator at 37°C (5% CO<sub>2</sub>, 95% air) for 24 h. Cells that migrated to the basement membrane were fixed with 4% paraformaldehyde and stained with crystal violet, observed under an IX73 microscope (Olympus) at 100 $\times$  magnification, and photographed using a DP80 Imaging system (Olympus). Numbers of migrated cells were counted in images of five independent fields.

## Karyotype analysis

ZX2021H cells (passage 30) were seeded in a 60-mm dish and incubated at 37°C with 5% CO<sub>2</sub>. When the cells reached 70% confluence, they were treated with 0.04 µg/ml colcemid (Thermo Fisher Scientific, Inc.) for 2 h to induce mitotic arrest. The cells were then collected, resuspended in 75 mM KCl for 20 min, fixed in methanol-acetic acid (3:1) for 10 min, and karyotyped. The cell suspension was dropped onto a moist, pretreated slide and incubated overnight at 70°C. The fixed cells were treated with 0.1% trypsin for 25 s at 37°C, rinsed twice with phosphate-buffered saline (PBS), stained with prewarmed (37°C) 3% Giemsa solution (pH 6.8) for 5 min, and the karyotype was determined according to the International System for Human Nomenclature (ISCN, 2020).

## Short tandem repeat profiling

Genomic DNA was extracted from the cultured cells (passage 30) for short tandem repeat (STR) DNA profiling. Briefly, genomic DNA was amplified by polymerase chain reaction (PCR) reaction and assayed using an ABI 3130XL DNA Analyzer (Applied Biosystems) to determine the STR loci. The STR profiles were then compared with the profiles in public cell banks, including the American Type Culture Collection (ATCC), Japanese Collection of Research Bioresources, and Deutsche Sammlung von Mikroorganismen und Zellkulturen GmbH, for reference. Twenty-one STR loci (D19S433, D5S818, D21S11, D18S51, D6S1043, AMEL, D3S1358, D13S317, D7S820, D16S539, CSF1PO, Penta D, D2S441, vWA, TPOX, Penta E, TH01, D12S391, D2S1338, and FGA) were matched for DNA fingerprinting analysis.

## In vivo tumorigenicity

We evaluated the in vivo tumorigenicity of the ZX2021H cell line by subcutaneous injection into mice. The mice were purchased from the Institute of Laboratory Animals Science, CAMS & PUMC (experimental animal license number SCXK2019-0008) and maintained under pathogen-free conditions and fed with sterilized food and autoclaved water. A cell suspension ( $5 \times 10^5$ ) was prepared in 200 µl of PBS with 100 µl Matrigel (BD Biosciences) and injected subcutaneously into the inguinal region on the right flank of 6-week-old female athymic BALB/c-nude mice ( $n = 5$ ). Tumor volume was measured in vivo every 3 days using Vernier calipers, and the experimental mice were euthanized after 30 days to determine the tumorigenicity.

## Real-time quantitative PCR analysis

Total RNA was extracted from cultured ZX2021H and H1299 cells (purchased from ATCC) using TRIzol reagent

(Invitrogen) following the manufacturer's instructions. Total RNA was reverse transcribed to cDNA using reverse transcription reagents (TaKaRa Bio) according to the manufacturer's instructions. SYBR Green premix (Vazyme) was combined with the cDNA templates to perform quantitative real time-polymerase chain reaction (qRT-PCR) using a 7900 Real-Time PCR System (Applied Biosystems). Each experiment was run in triplicate. All primers used in the experiment are shown in Table 1.

## Gene mutation screening

Genomic DNA samples of ZX2021H cells at passage 25 were screened for 69 specific genes mutations using next-generation sequencing (NGS) technology on an Illumina sequencing platform (Sino-us Diagnostics). The types of gene mutation contained point or frameshift mutation, sites of mutation (codon, exon, functional domain, or conserved area), copy number variants (CNVs), fusion variant, insertion and deletion mutations. The list of the 69 genes are shown in Table S1; Gene mutations of 12 commonly-used lung adenocarcinoma cell lines were obtained from the Cancer Cell Lines Encyclopedia (CCLE, <https://portals.broadinstitute.org/ccle>).

## Statistical analysis

All data were obtained from three independent experiments and analyzed using Student's *t*-tests (GraphPad Prism; GraphPad Software). The results are presented as mean  $\pm$  standard deviation. A *p*-value <0.05 was considered statistically significant.

## RESULTS

In the current study, we cultured clinical specimens resected from metastatic lymph node tissue using a specifically formulated McCoy's 5A medium to obtain a novel lung cancer cell line with high growth and metastatic potential suitable for studying lung cancer malignant progression. We then further established and characterized the ZX2021H cell line.

### Establishment of a novel lung cancer cell line ZX2021H

To establish a novel lung cancer cell line as described above, we harvested clinical metastatic lymph node tissue samples from a lung cancer patient (Figure 1a,b). Cells in primary culture were purified by enzymatic digestion and differential adherence, and a cell line was successfully established in vitro after freezing, resuscitating, and culturing in McCoy's 5A medium supplemented with 20% FBS for >50 generations. The cell line was designated ZX2021H.

**TABLE 1** The primers used in quantitative RT-PCR

Genes	Primers	Sequence (5'-3')
hGAPDH	Forward primer	GGAGCGAGATCCCTCCAAAAT
	Reverse primer	GGCTGTTGTCATACTTCTCATGG
hACC	Forward primer	TGAGACTAGCCAAACAATCTCTGT
	Reverse primer	AGAAAGTAGAAGCTCCGATCCT
hElovl6	Forward primer	AGCAGTCAGTTTGTGACCAGG
	Reverse primer	ATCTCTAGTTCGGGTGCTTT
hFASN	Forward primer	AAGGACCTGTCTAGTGTGATGC
	Reverse primer	TGGCTTCATAGGTGACTTCCA
hSCD	Forward primer	CACCCAGCTGTCAAAGAGAAG
	Reverse primer	AGGACGATATCCGAAGAGGTGG
hPGC-1 $\alpha$	Forward primer	GCTTCTGGGTGGACTCAAC
	Reverse primer	CTGCTAGCAAGTTTGCTCA
hPGC-1 $\beta$	Forward primer	CAGGCGATGGTGCAACTCATA
	Reverse primer	CAGAGCACGTCTTGAGCCA
hEsrra	Forward primer	GAGATCACCAAGCGGAGACG
	Reverse primer	ATGAGACACCAGTGCATTAC
hNRF1	Forward primer	AGGAACACGGAGTGACCCAA
	Reverse primer	TGCATGTGCTTCTATGGTAGC
hKlf2	Forward primer	TTCGGTCTCTTCGACGACG
	Reverse primer	TGCGAACTCTTGGGTAGGTC
hKlf4	Forward primer	ACCTACACAAAGAGTCCCATC
	Reverse primer	TGTGTTTACGGTAGTGCCTG
h4-Oct	Forward primer	CGAAAGAGAAAGCGAACCAG
	Reverse primer	GCCGGTTACAGAACCACACT
hSox2	Forward primer	TGGACAGTTACGCGCAT
	Reverse primer	CGAGTAGGACATGCTGTAGGT
hTbx3	Forward primer	GAGGCTAAAGAACTTTGGGATCA
	Reverse primer	CATTCGGGGTCGGCCTTA
hnr5a2	Forward primer	TCATGCTGCCAAAGTGGAGA
	Reverse primer	TGGTTTTGGACAGTTCGCTT
hEcadherin	Forward primer	CGAGAGCTACACGTTACCGG
	Reverse primer	GGGTGTCGAGGGAAAAATAGG
hSnail	Forward primer	GAGGCGGTGGCAGACTAG
	Reverse primer	GACACATCGGTCAGACCAG
hTwist	Forward primer	CGGGAGTCCGCAGTCTTA
	Reverse primer	TGAATCTTGCTCAGTTGTCT
hVimentin	Forward primer	GACGCCATCAACACCGAGTT
	Reverse primer	CTTTGTCGTTGGTTAGCTGGT
hFIH-1	Forward primer	GCCAGACCCACAAGTTCTT
	Reverse primer	CCTGTTGGACCTCGGCTTAA
hHIF-1 $\alpha$	Forward primer	AGTGTACCCTAACTAGCCGAGGAA
	Reverse primer	CTGAGGTTGGTTACTGTTGGTATCA
hPHD1	Forward primer	AACATCGAGCCACTCTTTGAC
	Reverse primer	TCCTTGGCATCAAAAATACCAG
hPHD2	Forward primer	AGATTGCCTGGGTGGAAG
	Reverse primer	TTGCCTGGGTAACACGCC
hPHD3	Forward primer	ATCAGTTCCTCCTGTGCC
	Reverse primer	CAGCGACCATCACCGTTG

(Continues)

**TABLE 1** (Continued)

Genes	Primers	Sequence (5'-3')
hP21	Forward primer	TGTCCGTCAGAACCCATGC
	Reverse primer	AAAGTCGAAGTTCCATCGCTC
hCCNA2	Forward primer	GCGCTGGCGGTACTGAAAGT
	Reverse primer	AGGAACGGTGACATGCTCATC
hCCNB1	Forward primer	CAGGTTGTTGCAGGAGACCAT
	Reverse primer	CCAGCTGCAGCATCTTCTTG
hCCND1	Forward primer	CTGGAGGTCTGCGAGGAACA
	Reverse primer	CTGCAGGCGGCTCTTTTTTC
hCCNE1	Forward primer	TGCTGCTTCGGCCTTGTATC
	Reverse primer	ATGGCAAATGGAACCATCCA
hCCNH	Forward primer	TGCATTGACGGATGCTTACC
	Reverse primer	CAGCCCTGGAGGCACTAGATA
hMYC	Forward primer	AGTGGAAAACCAGCAGCCTC
	Reverse primer	TTCTCTCCTCGTCGAGTA

## Characterization of the ZX2021H cell line

### Morphological characteristics of ZX2021H cell line

We periodically observed the morphology of ZX2021H cells under an inverted microscope during long-term cultivation in vitro (passage >50) (Figure 1c). The cells showed a consistent and well-differentiated morphology. Most cells were polygonal and others were fusiform. The cells also had a high nuclear-cytoplasm ratio. The morphology did not change significantly when the cells were maintained for 50 passages. Moreover, ZX2021H cells grew rapidly in monolayers and then overlapped and piled up at high densities when they covered the whole plate, indicating increased proliferation and malignant potential resulting from loss of contact inhibition.

### Proliferation characteristics of ZX2021H cell line in vitro

We evaluated the proliferation characteristics of ZX2021H cells by CCK8 and colony-formation methods. The cell growth curve of ZX2021H cells based on the CCK8 results is shown in Figure 1d. ZX2021H cells entered the logarithmic growth phase on the second day after seeding, with a population-doubling time of approximately 29.8 h. In addition, colony-formation assays further proved that ZX2021H cells had proliferative potential when seeded at 500 or 1000 cells (Figure 1e).

### Aggressive characteristics of ZX2021H cells

We investigated the aggressiveness of ZX2021H cells in invasion and migration assays using Transwell chambers



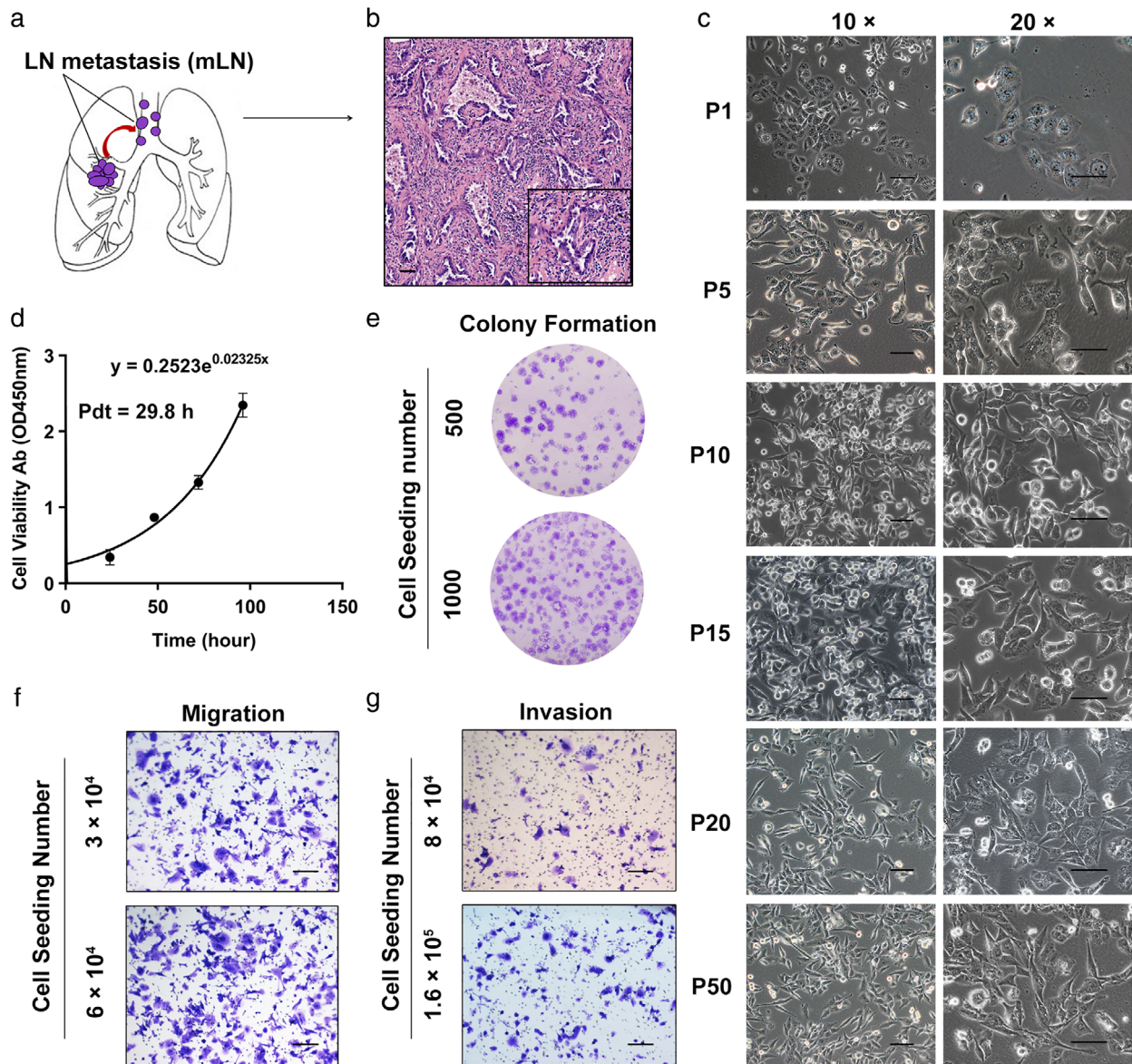


**FIGURE 1** Phenotypic characterization of ZX2021H cell line derived from a patient with lung adenocarcinoma and lymph node metastasis. (a) Overview of tissue origin. Tumor tissue was obtained from a metastatic lymph node (mLN) in a patient with lung adenocarcinoma. (b) Histopathological characteristics of primary tumor showing typical lung adenocarcinoma appearance. (c) Morphology of the ZX2021H cell line. Phase-contrast photomicrograph of ZX2021H cells at passages 1, 5, 10, 15, 20, 25, and 50 (10 $\times$  and 20 $\times$  magnification, respectively). Scale 100  $\mu$ m. (d) Proliferation of ZX2021H cells was evaluated by CCK-8 assay. (e) Colony formation of ZX2021H cells. (f) Colony formation was visualized microscopically at 14 days. (g) Migration and invasion analysis of ZX2021H cell line

with or without Matrigel. ZX2021H cells invaded through the Matrigel-coated basement membrane, especially when seeded at  $1.6 \times 10^5$  cells, indicating their potential invasion ability (Figure 1f,g). Moreover, ZX2021H cells also displayed prominent migration ability, even when seeded at  $3 \times 10^4$  cells. These results revealed that the ZX2021H cell line had highly aggressive characteristics, making it a suitable cell model for studying lung cancer malignant progression.

### Unique features of ZX2021H cell line: Cell line authentication and karyotype analysis

We genotyped the ZX2021H cell line to exclude the possibility of cross-contamination with other cell lines. We tested 21 STR loci (D19S433, D5S818, D21S11, D18S51, D6S1043, AMEL, D3S1358, D13S317, D7S820, D16S539, CSF1PO, D2S441, vWA, TPOX, TH01, D12S391, D2S1338). ZX2021H cells had a unique STR profile (Figure 2a,b), indicating that

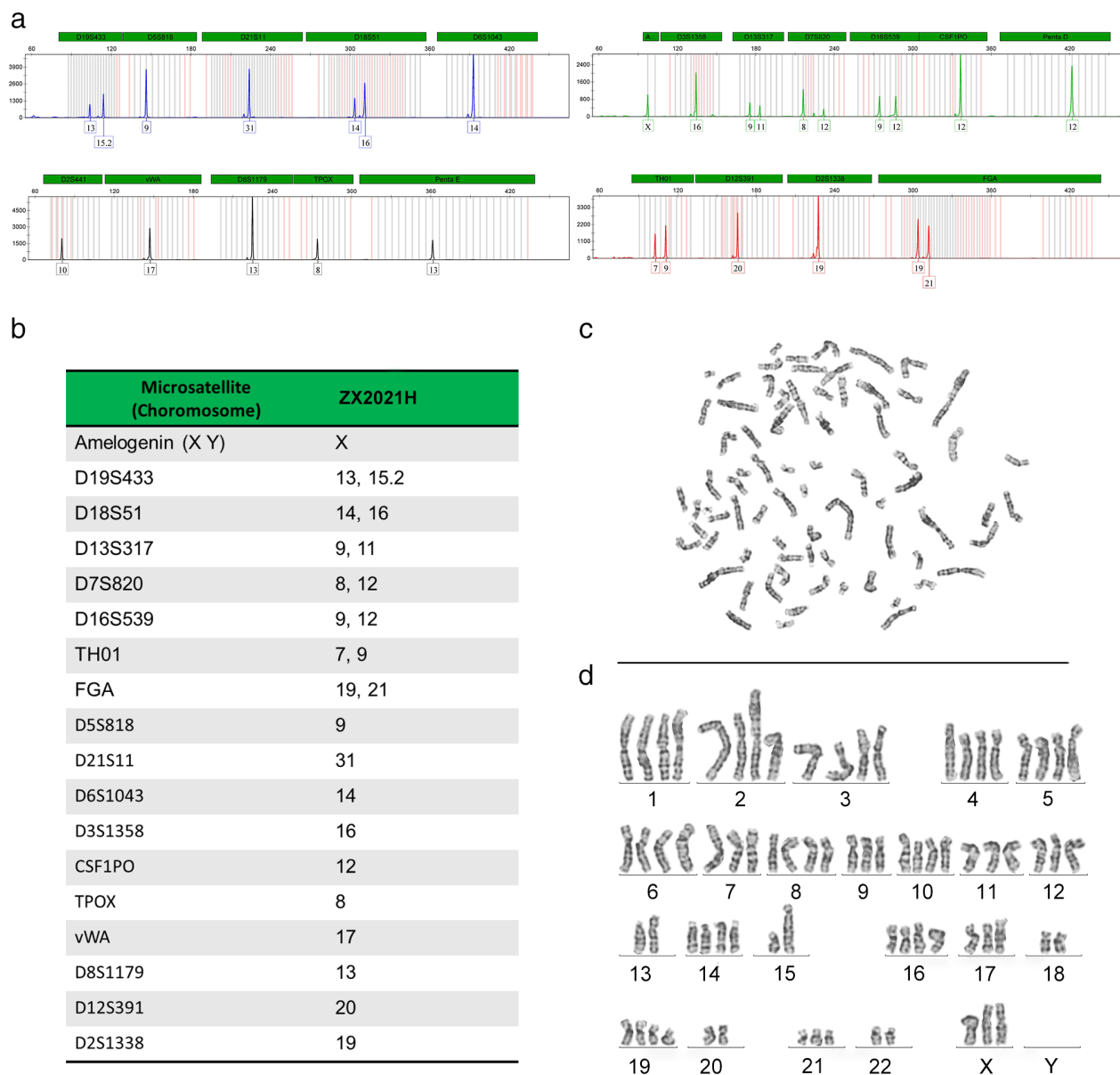


**FIGURE 2** Analysis of unique STR genotype profile and karyotype of ZX2021H cells. (a, b) Unique STR genotype profile of ZX2021H cell line. An electropherogram of the STR analysis was performed to confirm that the ZX2021H cell line differed from other known established human cell lines. (c, d) Representative G-banded metaphase of ZX2021H cell line. ZX2021H cell line at passage 30 was used for analysis. STR, short tandem repeat

we had established a novel lung cancer cell line. We also performed karyotype analysis to confirm the abnormalities. The ZX2021H cell line had 75 chromosomes (Figure 2c,d) and exhibited high chromosomal heterogeneity among cells (data not shown). Gross chromosomal abnormalities often confer indefinite cell growth potential, implying high malignancy.

### Proliferation characteristics of ZX2021H cell line in vivo

Furthermore, we also established a tumor xenograft model by subcutaneous injection of ZX2021H cells to evaluate their tumorigenic ability. Visible subcutaneous xenografts with

rapid growth were detected after 3 weeks, with diameters of 0.5–1.5 cm at 4 weeks in all (5/5, 100%) nude mice (Figure 3e–i). These results demonstrated that ZX2021H cells had vigorous growth capabilities both in vitro and in vivo.

### Comparison of proliferation, migration, and invasion capabilities between ZX2021H and H1299 cells in vitro and in vivo

The H1299 cell line, previously derived from metastatic lymph node tissue from a lung cancer patient, had the properties of unlimited proliferation and aggressive migration and invasion, consistent with the characteristics of the

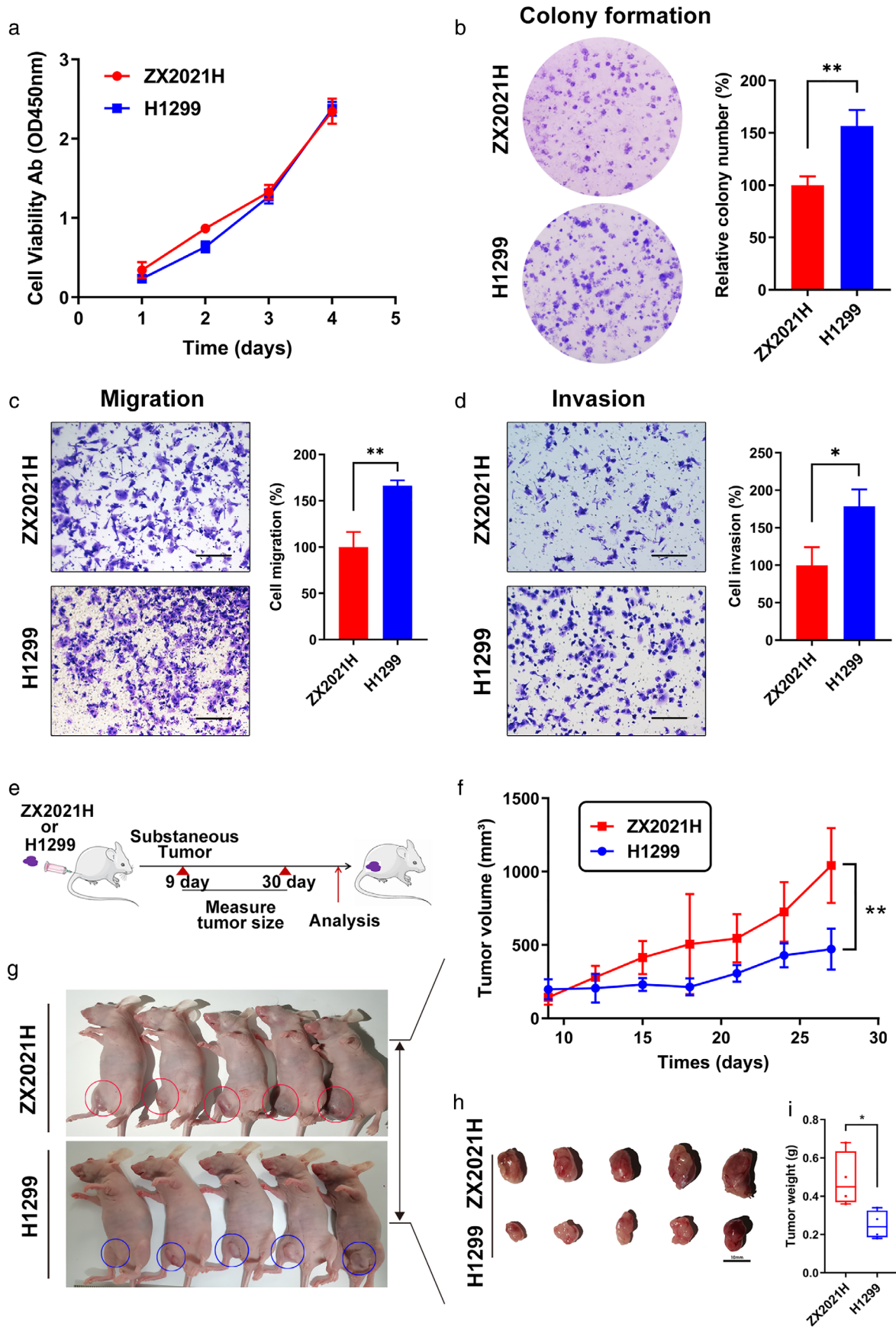
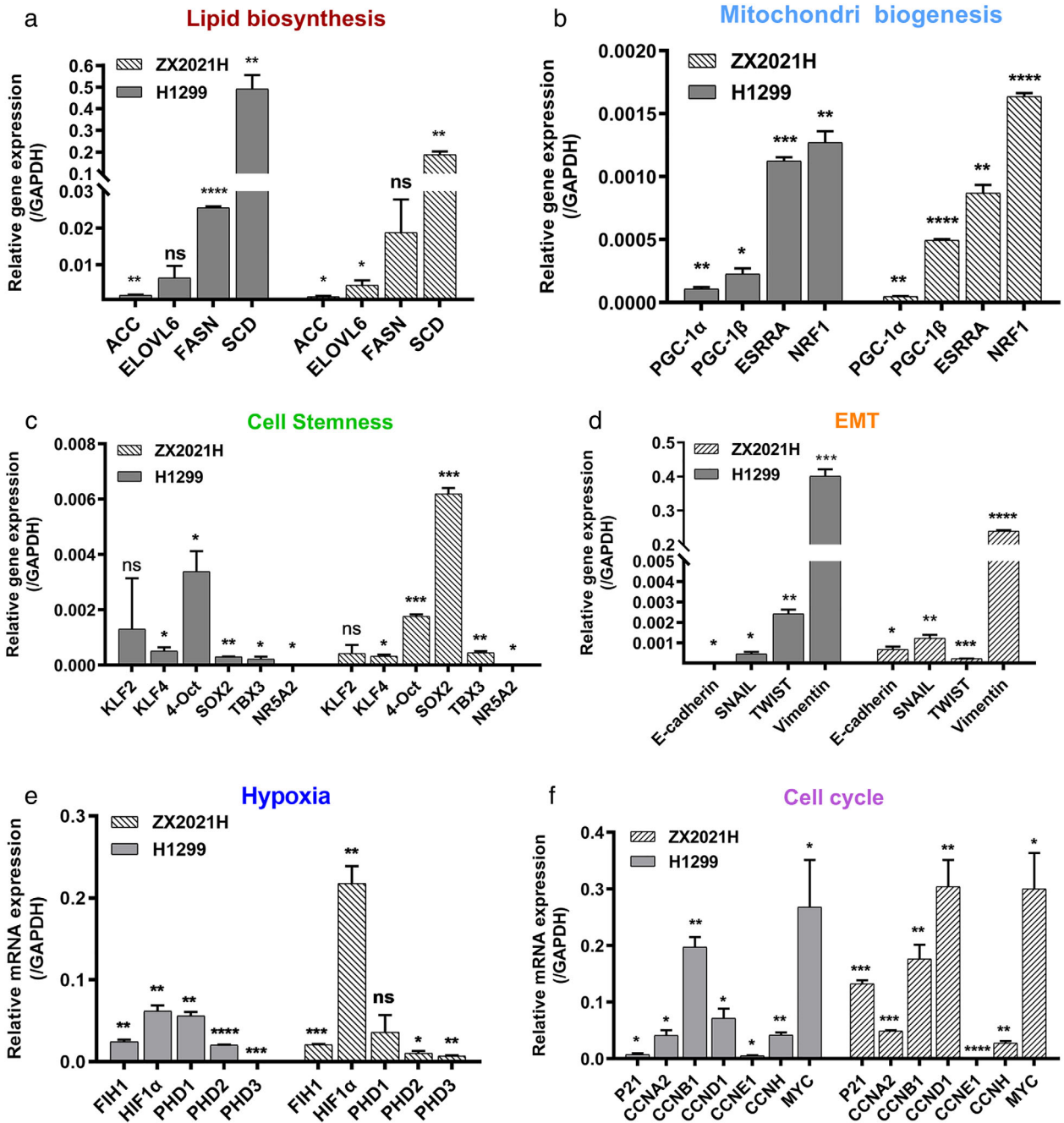


FIGURE 3 Legend on next page.





**FIGURE 4** Expression levels of genes related to cell stemness, EMT, lipid biosynthesis, mitochondria biogenesis, hypoxia, and the cell cycle in ZX2021H and H1299 cells. Expression levels of (a) lipid biosynthesis-associated genes, (b) mitochondria biogenesis-associated genes, (c) stem cell-associated genes, and (d) EMT-associated genes in ZX2021H and H1299 cells. (e) Analysis of the expression level of hypoxia-associated genes; (f) analysis of the expression level of cell cycle-associated genes in ZX2021H and H1299 cells. All data presented as mean ± SD of triplicate assays and represent one of two independent experiments. \**p* < 0.05, \*\**p* < 0.01, \*\*\**p* < 0.001. EMT, epithelial-mesenchymal transition

**FIGURE 3** Proliferation, migration, and invasion abilities of ZX2021H and H1299 cells in vitro and in vivo. (a) The proliferation abilities of ZX2021H and H1299 cells were assessed by CCK8 assay. (b) Colony-formation abilities of ZX2021H and H1299 cells. (c, d) Cell migration and invasion activities of ZX2021H and H1299 cells using Transwell chambers and Matrigel-coated Transwell chambers assays, respectively. (e) Experimental flowchart for (f–i). ZX2021H or H1299 cells were injected subcutaneously into nude mice (*n* = 9 mice per group). (f, g) Subcutaneous ZX2021H and H1299 tumors were measured every 2 days after tumor-cell injection and the size was calculated using the formula: Tumor size (mm<sup>3</sup>) = [(length) × (width)<sup>2</sup>]/2. Data are presented as mean ± SD of samples (*n* = 9). (h) Representative images of tumor volumes from ZX2021H- and H1299 tumor-bearing nude mice. (i) Representative images of subcutaneous tumor weights

ZX2021H cell line, indicating that it would provide an ideal model for investigating lung cancer malignant progression.<sup>24–26</sup> We further evaluated the feasibility of ZX2021H cells as a suitable model for investigating lung cancer malignant progression by comparing its proliferation, migration, and invasion capabilities with the H1299 cell line. We assessed the proliferation capabilities of the two cell lines using CCK8 and colony-formation assays. CCK8 assay showed that ZX2021H cells had a similar vigorous growth tendency to H1299 cells (Figure 3a) but a weaker colony-formation ability (Figure 3b). Moreover, ZX2021H cells had slightly weaker migration and invasion capabilities than H1299 cells according to Transwell assays, but remained highly aggressive (Figure 3c,d).

We also identified the tumorigenic abilities of ZX2021H and H1299 cells in nude mice in vivo. Tumor formation was observed on the ninth day after inoculation, showing 100% tumorigenicity (Figure 3e,f). Xenograft tumors established with ZX2021H cells exhibited faster growth than tumors from H1299 cells, but there was no difference in proliferation between ZX2021H and H1299 cells in vitro (Figure 3g–i). However, no tumor metastases were observed during follow-up in either of the models. This may be because the xenograft study did not allow enough time for tumor metastasis. This issue therefore needs to be investigated in further studies.

## Gene signatures of ZX2021H and H1299 cell lines

Increasing research has reported that the biological processes of lipid biosynthesis,<sup>27</sup> mitochondria biogenesis,<sup>28</sup> cell stemness,<sup>29</sup> epithelial-mesenchymal transition (EMT),<sup>30</sup> hypoxia,<sup>31</sup> and the cell cycle<sup>32</sup> play pivotal roles in tumor malignant progression. We explored the causes for the different biological characteristics of ZX2021H and H1299 cells by examining the expression levels of relevant genes. *SOX2* expression levels were significantly higher in ZX2021H compared with H1299 cells (Figure 4c), explaining the higher growth rate of ZX2021H compared with H1299 cells in vivo. Furthermore, *HIF1 $\alpha$*  and *CCND1* expression levels were also significantly upregulated in ZX2021H compared with H1299 cells (Figure 4e,f), but there was no significant difference in the expression levels of other genes related to lipid biosynthesis,<sup>27</sup> mitochondria biogenesis and EMT (Figure 4a,b,d,f).

## Gene mutations in ZX2021H cells

Here, we detected the cancer-related critical genes mutation status in ZX2021H cells. Screening by NGS, we found four cancer-related gene mutations (NF1, TP53, BRAF, and

**TABLE 2** Four cancer-related gene mutations in ZX2021H cells screened by next-generation sequencing (NGS)

Gene	Position	CDS mutation	AA mutation	Type
NF1	chr17, Exon42	c.6398_6399del	p.L2133fs	Deletion-frameshift
TP53	chr17, Exon5	c.536A>G	p.H179R	Substitution-missense
BRAF	chr7, Exon1	c.64G>A	p.D22N	Substitution-missense
MET	chr7, 116312557_116436239	exon1-exon21	14.16copies	Copy number variants (CNV)

**TABLE 3** Comparison of mutation status of cancer critical genes in ZX2021H and 12 commonly-used LUAD cell lines

Cell line	APC	ALK	BRAF	K-RAS	EGFR	MET	NF1	PIK3CA	TP53	PTEN	MSH2
ZX2021H	wt	wt	p.D22N	wt	wt	CNV	p.L2133fs	wt	p.H179R	wt	wt
A549	wt	wt	wt	p.G12S	wt	wt	wt	wt	wt	wt	wt
NCI-H2030	wt	wt	wt	p.G12C	wt	wt	p.T2444T	wt	p.G262V	wt	wt
NCI-H1975	p.S2134C	wt	wt	wt	p.T745M	wt	wt	p.G118D	p.R273H	wt	wt
NCI-H2228	wt	wt	wt	wt	wt	wt	wt	wt	p.Q331*	wt	wt
NCI-H2122	wt	wt	wt	p.G12C	wt	wt	wt	wt	p.C176F p.Q16L	wt	wt
NCI-H23	wt	p.L1035L	wt	p.G12C	wt	wt	wt	wt	p.M246I	wt	wt
Calu-3	wt	wt	wt	wt	wt	wt	wt	wt	p.C277F p.M237I	wt	wt
PC9	wt	p.E1299K	wt	wt	p.ELREA701del	wt	wt	wt	wt	wt	wt
NCI-H3255	wt	wt	wt	wt	p.L813R	wt	wt	wt	NA	wt	wt
NCI-H3122	wt	wt	wt	wt	wt	wt	p.I1824V	wt	p.E285V	wt	wt
NCI-H1792	wt	wt	wt	p.G12C	wt	wt	wt	wt	wt	wt	wt
NCI-H1435	wt	p.G744R	wt	wt	wt	wt	p.K615N	wt	p.C141W	wt	wt



MET) (Table 2). A frameshift mutation in exon 42 of NF1 gene was detected, which caused the disruption of reading frame and meant the inactivation of NF1 function. A missense mutation in exon 5 of TP53 gene (p.H179R) and in exon 1 of BRAF gene (p.D22N) was detected, respectively. Moreover, copy number variants were found in MET. We also compared the mutation status of cancer-related critical genes in ZX2021H cells with that in 12 commonly-used lung adenocarcinoma (LUAD) cell lines, and it was shown that ZX2021H with BRAF (p.D22N), NF1 (p.L2133fs) and MET (CNV) mutations was a unique lung adenocarcinoma cell line (Table 3).

## DISCUSSION

Suitable *ex vivo* cell models are urgently needed to support clinical and fundamental research into lung cancer. Cell models allow the possible effects of new antitumor drugs and gene functions to be assessed by detecting phenotype changes following drug treatment or gene transfection, respectively. Although >20 lung cancer cell lines are available in the ATCC cell bank, most are derived from primary lesions and are thus optimized for investigating tumorigenicity and the development of new anticancer drugs, rather than for research into metastatic mechanisms. It is therefore necessary to establish a high metastatic potential lung cancer cell line derived from metastatic lesions, which would be more suitable for revealing the underlying metastatic mechanisms in lung cancer.

In the present study, we successfully established and characterized a novel NSCLC cell line (ZX2021H) derived from metastatic lymph node tissue from a Chinese patient with advanced NSCLC. The established cell line, ZX2021H, showed prominent capacities for constant proliferation and invasion *in vitro*, because the cells had already undergone distant metastasis in the patient, thus conferring their potential aggressive ability and vigorous growth tendency. Similarly, the H1299 cell line with high proliferation and aggressive capabilities was derived from metastatic lymph node tissue from a lung cancer patient, and thus provided an ideal model for investigating the tumorigenicity and metastasis of lung cancer. Compared with H1299 cells, ZX2021H cells demonstrated greater tumorigenic capability *in vivo*, making them more suitable for functional experiments designed to screen new anticancer drugs and evaluate genes of interest *in vivo*. However, no metastatic nodes were observed with either cell line during follow-up in an *in vivo* xenograft model, possibly because the follow-up time was too short to detect tumor metastasis. This needs to be confirmed in further studies. Moreover, the coexistence of irregular polygonal and fusiform cell morphologies suggested that the ZX2021H cell line had a polyclonal origin. Karyotype analysis revealed evident numerical and structural chromosome abnormalities, implying a high malignant potential of the ZX2021H cell line. Overall, the ZX2021H cell line was shown to be a potentially ideal cell model

for exploring the molecular mechanisms underlying lung cancer metastasis and for testing novel molecularly targeted therapeutics.

Emerging research has indicated pivotal roles for lipid biosynthesis,<sup>27</sup> mitochondria biogenesis,<sup>28</sup> cell stemness,<sup>29</sup> EMT,<sup>30</sup> hypoxia,<sup>31</sup> and the cell cycle<sup>32</sup> in tumor malignant progression. We therefore evaluated the expression levels of genes related to these biological processes in ZX2021H and H1299 cell lines. We found no difference in the expression of genes associated with lipid biosynthesis, mitochondria biogenesis, and EMT between the two cell lines. However, SOX2 expression was enhanced in ZX2021H cells when compared with H1299 cells. Previous studies have shown that SOX2 is related to cell stemness and plays a critical role in the progression, metastasis and chemoresistance of tumor cells. Hernando et al. mentioned that SOX2 is responsible for glioblastoma cell stemness and tumor propagation,<sup>33</sup> and elevated SOX2 expression has been linked to malignant cell behavior in lung cancer.<sup>34,35</sup> A recent study in prostate cancer cells also point to SOX2 as the main regulator of metabolic reprogramming.<sup>36</sup> Accordingly, the aforementioned studies raise the possibility that high level of SOX2 may lead to the rapid growth rate of ZX2021H cells *in vivo* compared with H1299 cells.

The cell line models with a clear genetic background are important in the study of targeted drug and precision medicine. Screening by NGS, we detected four cancer-related gene mutations (NF1, TP53, BRAF, and MET), of which, NF1 is a negative regulator of the ras signal transduction pathway and a frameshift mutation in exon 42 predicted the inactivation of NF1 function, which in turn will result in the aberrant activation of the ras signal transduction pathway.<sup>37,38</sup> Solomon et al. mentioned that TP53 mutant (p.H179R) induces a unique expression pattern of a cancer-related gene signature (CGS) by elevating H-Ras activity.<sup>39</sup> However, the protein function of BRAF caused by the mutation (p.D22N) was unknown, so as the MET (CNV). Furthermore, comparing the mutation status of cancer-related critical genes in ZX2021H with that in 12 commonly-used LUAD cell lines, ZX2021H cell line is a unique cell line with BRAF (p.D22N), NF1 (p.L2133fs) and MET (CNV) mutations, which enriches the diversity of LUAD cell lines.

In conclusion, the ZX2021H cell line had a higher proliferation ability *in vivo* and higher expression of the cell stemness-related gene SOX2 compared with H1299 cells, which have been considered to have among the highest proliferation and aggressive capabilities of all lung cancer cell lines. We therefore identified the ZX2021H cell line as a highly malignant lung cancer cell line.

## ACKNOWLEDGEMENTS

This study was partly supported by the grants from Startup Project of Tianjin Lung Cancer Institute (No. TJLCZJ2021-09), Key Project of Tianjin Lung Cancer Institute (No. TJLCZD2021-05), and The Key Project of Cancer Foundation of China (No. CFC2020kyxm003), and the General Project of Tianjin Lung Cancer Institute (No. TJLCMS2021-03), and

Incubation Fund of General Hospital of Tianjin Medical University (No. ZYYFY2019022), and The present study was funded by the National Natural Science Foundation of China (No. 82172776).

## CONFLICT OF INTEREST

We declare that we have no conflict of interest.

## ORCID

Lingling Zu  <https://orcid.org/0000-0002-6976-6579>

Song Xu  <https://orcid.org/0000-0001-6153-387X>

## REFERENCES

- Sung H, Ferlay J, Siegel RL, Laversanne M, Soerjomataram I, Jemal A, et al. Global cancer statistics 2020: GLOBOCAN estimates of incidence and mortality worldwide for 36 cancers in 185 countries. *CA Cancer J Clin.* 2021;71(3):209–49.
- Siegel RL, Miller KD, Fuchs HE, Jemal A. Cancer statistics, 2021. *CA Cancer J Clin.* 2021;71(1):7–33.
- Bajbouj K, Al-Ali A, Ramakrishnan RK, et al. Histone modification in NSCLC: molecular mechanisms and therapeutic targets. *Int J Mol Sci.* 2021;22(21):11701.
- Herbst RS, Morgensztern D, Boshoff C. The biology and management of non-small cell lung cancer. *Nature.* 2018;553(7689):446–54.
- Miller M, Hanna N. Advances in systemic therapy for non-small cell lung cancer. *BMJ.* 2021;375:n2363.
- Saw SPL, Ong BH, Chua KLM, Takano A, Tan DSW. Revisiting neo-adjuvant therapy in non-small-cell lung cancer. *Lancet Oncol.* 2021;22(11):e501–16.
- Shang S, Liu J, Verma V, Wu M, Welsh J, Yu J, et al. Combined treatment of non-small cell lung cancer using radiotherapy and immunotherapy: challenges and updates. *Cancer Commun (Lond).* 2021;41:1086–99.
- Ko J, Winslow MM, Sage J. Mechanisms of small cell lung cancer metastasis. *EMBO Mol Med.* 2021;13(1):e13122.
- Fisher ER, Paulson JD. A new in vitro cell line established from human large cell variant of oat cell lung cancer. *Cancer Res.* 1978;38(11 Pt 1):3830–5.
- Sugita M, Geraci M, Gao B, Powell RL, Hirsch FR, Johnson G, et al. Combined use of oligonucleotide and tissue microarrays identifies cancer/testis antigens as biomarkers in lung carcinoma. *Cancer Res.* 2002;62(14):3971–9.
- Welsh S, Williams R, Kirkpatrick L, Paine-Murrieta G, Powis G. Antitumor activity and pharmacodynamic properties of PX-478, an inhibitor of hypoxia-inducible factor-1 $\alpha$ . *Mol Cancer Ther.* 2004;3(3):233–44.
- Chen C, Akerstrom V, Baus J, Lan MS, Breslin MB. Comparative analysis of the transduction efficiency of five adeno associated virus serotypes and VSV-G pseudotype lentiviral vector in lung cancer cells. *Virology.* 2013;54:86.
- Qin X, Yu S, Zhou L, Shi M, Hu Y, Xu X, et al. Cisplatin-resistant lung cancer cell-derived exosomes increase cisplatin resistance of recipient cells in exosomal miR-100-5p-dependent manner. *Int J Nanomed.* 2017;12:3721–33.
- Zhang Y, Wang X, Han L, Zhou Y, Sun S. Green tea polyphenol EGCG reverse cisplatin resistance of A549/DDP cell line through candidate genes demethylation. *Biomed Pharmacother.* 2015;69:285–90.
- Ai C, Ma G, Deng Y, Zheng Q, Gen Y, Li W, et al. Nm23-H1 inhibits lung cancer bone-specific metastasis by upregulating miR-660-5p targeted SMARCA5. *Thorac Cancer.* 2020;11(3):640–50.
- Choi SJ, Lee H, Choe C, Shin YS, Lee J, Moon SH, et al. Establishment and characterization of a lung cancer cell line, SMC-L001, from a lung adenocarcinoma. *In Vitro Cell Dev Biol Anim.* 2014;50(6):519–26.
- Jiang Y, Zhao J, Zhang Y, Li K, Li T, Chen X, et al. Establishment of lung cancer patient-derived xenograft models and primary cell lines for lung cancer study. *J Transl Med.* 2018;16(1):138.
- Zheng C, Sun YH, Ye XL, Chen HQ, Ji HB. Establishment and characterization of primary lung cancer cell lines from Chinese population. *Acta Pharmacol Sin.* 2011;32(3):385–92.
- Tai AL, Fang Y, Sham JS, Deng W, Hu L, Xie D, et al. Establishment and characterization of a human non-small cell lung cancer cell line. *Oncol Rep.* 2005;13(6):1029–32.
- Sharifzadeh S, Owji SM, Pezeshki AM, Malek-Hoseini Z, Kumar PV, Ghayumi SMA, et al. Establishment and characterization of a human large cell lung cancer cell line with neuroendocrine differentiation. *Pathol Oncol Res.* 2004;10(4):225–30.
- Yokouchi H, Yamazaki K, Asahina H, Shigemura M, Moriyama T, Takaoka K, et al. Establishment and characterization of amylase-producing lung adenocarcinoma cell line, IMEC-2. *Anticancer Res.* 2006;26(4B):2821–7.
- Masuda N, Fukuoka M, Takada M, Kudoh S, Kusunoki Y. Establishment and characterization of 20 human non-small cell lung cancer cell lines in a serum-free defined medium (ACL-4). *Chest.* 1991;100(2):429–38.
- Zou CY, Wang J, Shen JN, et al. Establishment and characteristics of two syngeneic human osteosarcoma cell lines from primary tumor and skip metastases. *Acta Pharmacol Sin.* 2008;29(3):325–32.
- Teng JF, Mei QB, Zhou XG, Tang Y, Xiong R, Qiu WQ, et al. Polyphyllin VI induces caspase-1-mediated pyroptosis via the induction of ROS/NF- $\kappa$ B/NLRP3/GSDMD signal axis in non-small cell lung cancer. *Cancers (Basel).* 2020;12(1):193.
- Chen Y, Tang Y, Tang Y, Yang Z, Ding G. Serine protease from *Nereis virens* inhibits H1299 lung cancer cell proliferation via the PI3K/AKT/mTOR pathway. *Mar Drugs.* 2019;17(6):366.
- Kim MJ, Park J, Kim J, Kim JY, An MJ, Shin GS, et al. Transcriptome analysis reveals HgCl<sub>2</sub> induces apoptotic cell death in human lung carcinoma H1299 cells through Caspase-3-independent pathway. *Int J Mol Sci.* 2021;22(4):2006.
- Vriens K, Christen S, Parik S, Broekaert D, Yoshinaga K, Talebi A, et al. Evidence for an alternative fatty acid desaturation pathway increasing cancer plasticity. *Nature.* 2019;566(7744):403–6.
- Lin S, Huang C, Sun J, Bollt O, Wang X, Wang X, Martine E, et al. The mitochondrial deoxyguanosine kinase is required for cancer cell stemness in lung adenocarcinoma. *EMBO Mol Med.* 2019;11(12):e10849.
- Li C, Zhang J, Yang X, Hu C, Chu T, Zhong R, et al. hsa\_circ\_0003222 accelerates stemness and progression of non-small cell lung cancer by sponging miR-527. *Cell Death Dis.* 2021;12(9):807.
- Pan J, Fang S, Tian H, Zhou C, Zhao X, Tian H, et al. lncRNA JPX/miR-33a-5p/Twist1 axis regulates tumorigenesis and metastasis of lung cancer by activating Wnt/beta-catenin signaling. *Mol Cancer.* 2020;19(1):9.
- Shi Y, Fan S, Wu M, Zuo Z, Li X, Jiang L, et al. YTHDF1 links hypoxia adaptation and non-small cell lung cancer progression. *Nat Commun.* 2019;10(1):4892.
- Sheng H, Lv W, Zhu L, Wang L, Wang Z, Han J, et al. Liriopesides B induces apoptosis and cell cycle arrest in human non-small cell lung cancer cells. *Int J Mol Med.* 2020;46(3):1039–50.
- Lopez-Bertoni H, Johnson A, Rui Y, Lal B, Sall S, Malloy M, et al. Sox2 induces glioblastoma cell stemness and tumor propagation by repressing TET2 and deregulating 5hmC and 5mC DNA modifications. *Signal Transduct Target Ther.* 2022;7(1):37.
- Wang K, Ji W, Yu Y, et al. FGFR1-ERK1/2-SOX2 axis promotes cell proliferation, epithelial-mesenchymal transition, and metastasis in FGFR1-amplified lung cancer. *Oncogene.* 2018;37(39):5340–54.
- Zhu Y, Huang S, Chen S, Chen J, Wang Z, Wang Y, et al. SOX2 promotes chemoresistance, cancer stem cells properties, and epithelial-mesenchymal transition by  $\beta$ -catenin and Beclin1/autophagy signaling in colorectal cancer. *Cell Death Dis.* 2021;12(5):449.
- de Wet L, Williams A, Gillard M, Kregel S, Lamperis S, Gutgesell LC, et al. SOX2 mediates metabolic reprogramming of prostate cancer cells. *Oncogene.* 2022;41(8):1190–202.
- Arai H, Elliott A, Millstein J, Xiu J, Ou FS, Innocenti F, et al. Molecular characteristics and clinical outcomes of patients with Neurofibromin 1-altered metastatic colorectal cancer. *Oncogene.* 2022;41(2):260–7.

38. Pan Y, Hysinger JD, Barron T, Schindler NF, Cobb O, Guo X, et al. NF1 mutation drives neuronal activity-dependent initiation of optic glioma. *Nature*. 2021;594(7862):277–82.
39. Solomon H, Buganim Y, Kogan-Sakin I, Pomeraniec L, Assia Y, Madar S, et al. Various p53 mutant proteins differently regulate the Ras circuit to induce a cancer-related gene signature. *J Cell Sci*. 2012;125(Pt 13):3144–52.

### SUPPORTING INFORMATION

Additional supporting information may be found in the online version of the article at the publisher's website.

**How to cite this article:** Zu L, Li X, He J, Zhou N, Meng F, Li X, et al. Establishment and characterization of a novel highly malignant lung cancer cell line ZX2021H derived from a metastatic lymph node lesion. *Thorac Cancer*. 2022;13:1199–210. <https://doi.org/10.1111/1759-7714.14385>